3′ Phosphatase activity toward phosphatidylinositol 3,4-bisphosphate [PI(3,4)P_2] by voltage-sensing phosphatase (VSP)

Tatsuki Kurokawa[a,1], Shunsuke Takasuga[b], Souhei Sakata[a], Shinji Yamaguchi[c], Shigeo Horie[d], Koichi J. Homma[c], Takehiko Sasaki[b], and Yasushi Okamura[a,e,2]

[a]Laboratory of Integrative Physiology, Graduate School of Medicine, Osaka University, Suita, Osaka 565-0871, Japan; [b]Department of Medical Biology, Graduate School of Medicine, Akita University, Akita 010-8543, Japan; [c]Department of Molecular Biology, Faculty of Pharmaceutical Sciences, Teikyo University, Itabashi-ku, Tokyo 173-8605, Japan; [d]Department of Urology, School of Medicine, Teikyo University, Itabashi-ku, Tokyo 173-8605, Japan; and [e]Graduate School of Frontier Bioscience, Osaka University, Suita, Osaka 565-0871, Japan

Edited* by Gail Mandel, Howard Hughes Medical Institute and Oregon Health and Science University, Portland, OR, and approved April 27, 2012 (received for review March 4, 2012)

Voltage-sensing phosphatases (VSPs) consist of a voltage-sensor domain and a cytoplasmic region with remarkable sequence similarity to phosphatase and tensin homolog deleted on chromosome 10 (PTEN), a tumor suppressor phosphatase. VSPs dephosphorylate the 5′ position of the inositol ring of both phosphatidylinositol 3,4,5-trisphosphate [PI(3,4,5)P_3] and phosphatidylinositol 4,5-bisphosphate [PI(4,5)P_2] upon voltage depolarization. However, it is unclear whether VSPs also have 3′ phosphatase activity. To gain insights into this question, we performed in vitro assays of phosphatase activities of *Ciona intestinalis* VSP (Ci-VSP) and transmembrane phosphatase with tensin homology (TPTE) and PTEN homologous inositol lipid phosphatase (TPIP; one human ortholog of VSP) with radiolabeled PI(3,4,5)P_3. TLC assay showed that the 3′ phosphate of PI(3,4,5)P_3 was not dephosphorylated, whereas that of phosphatidylinositol 3,4-bisphosphate [PI(3,4)P_2] was removed by VSPs. Monitoring of PI(3,4)P_2 levels with the pleckstrin homology (PH) domain from tandem PH domain-containing protein (TAPP1) fused with GFP (PH_{TAPP1}-GFP) by confocal microscopy in amphibian oocytes showed an increase of fluorescence intensity during depolarization to 0 mV, consistent with 5′ phosphatase activity of VSP toward PI(3,4,5)P_3. However, depolarization to 60 mV showed a transient increase of GFP fluorescence followed by a decrease, indicating that, after PI(3,4,5)P_3 is dephosphorylated at the 5′ position, PI(3,4)P_2 is then dephosphorylated at the 3′ position. These results suggest that substrate specificity of the VSP changes with membrane potential.

phosphoinositide | ascidian

Phosphoinositides serve as not only components of biological membranes, but also as coordinators of diverse cellular events including proliferation, cell migration, vesicle turnover, and ion transport. Numerous phosphatases and kinases that regulate phosphoinositide availability have been identified (1, 2), and defects or enhancements of these enzymes lead to tumorigenesis, metabolic disorders, and degeneration. Phosphatase and tensin homolog deleted on chromosome 10 (PTEN) is a well-characterized phosphatase that dephosphorylates phosphatidylinositol 3,4,5-trisphosphate [PI(3,4,5)P_3] (3). Defect or loss of PTEN leads to generation or progression of tumors (4, 5), and enhancement of PTEN underlies diabetes (6). We have shown that a sea squirt ortholog of one PTEN-related phosphatase, transmembrane phosphatase with tensin homology (TPTE)/TPTE and PTEN homologous inositol lipid phosphatase (TPIP), designated as *Ciona intestinalis* VSP (Ci-VSP), dephosphorylates phosphoinositides that depend on membrane potential (7, 8). Ci-VSP has a voltage-sensor domain (VSD) consisting of four transmembrane segments and a PTEN-like region. Despite its sequence similarity to PTEN in its active center, Ci-VSP exhibits 5′ phosphatase activity toward PI(3,4,5)P_3 and phosphatidylinositol 4,5-bisphosphate [PI(4,5)P_2], unlike PTEN. Such distinct substrate specificity from PTEN partly depends on two critical amino acids in the substrate-binding region (9, 10). Ci-VSP shows voltage-dependent enzyme activity; depolarization-induced motion of the VSD activates dephosphorylation of the 5′ (D5) phosphate from PI(4,5)P_2 and PI(3,4,5)P_3. Zebrafish and *Xenopus* orthologs of voltage-sensing phosphatase (VSP) also have similar properties (11, 12). TPTE, TPTE2, PTEN2, or TPIP, mammalian orthologs of VSP, have been demonstrated to function as phosphoinositide phosphatases (13–15). VSP/TPTE/TPIP is expressed in testis (7), epithelium of developing organs (16), and the nervous system (8). However, its biological role still remains elusive. To understand the biological functions of VSPs, it is crucial to understand the detailed relationship between profiles of phosphoinositides and voltage-dependent activities of VSP. Here we find that Ci-VSP and the orthologs have significant 3′ (D3) phosphatase activity toward phosphatidylinositol 3,4-bisphosphate [PI(3,4)P_2], and the level of PI(3,4)P_2 changes bidirectionally depending on the membrane voltage.

Results

3′ Phosphatase Activity of VSP in Vitro. Previous studies showed that Ci-VSP dephosphorylates the 5′ phosphate of the inositol ring of PI(3,4,5)P_3 and PI(4,5)P_2 (17, 18). However, it remains unknown whether Ci-VSP dephosphorylates the 3′ phosphate from PI(3,4,5)P_3 because phosphatase activity of Ci-VSPs toward PI(4,5)P_2 could have masked potential 3′ phosphatase activity toward PI(3,4,5)P_3 in previous studies. To address this issue, the cytoplasmic region of Ci-VSP or TPIP (the human VSP ortholog) was reacted with PI(3,4,5)P_3 that had a radiolabeled phosphate on the 3′, 4′, or 5′ (D3, D4, or D5) position of the inositol ring. The number of phosphoinositides with distinct numbers of phosphates was quantified by TLC. When the 4′ phosphate on the inositol ring of PI(3,4,5)P_3 was labeled with ^{32}P, radioactive signal appeared at the position corresponding to phosphatidylinositol monophosphate, indicating that both the D3 position phosphate and the D5 position phosphate were removed from PI(3,4,5)P_3 (Fig. 1*A*). PI(3,4,5)P_3 with radioactive phosphate

Author contributions: T.K., S.H., K.J.H., T.S., and Y.O. designed research; T.K., S.T., S.S., S.Y., and Y.O. performed research; T.K., S.T., S.S., and S.Y. analyzed data; and T.S. and Y.O. wrote the paper.

The authors declare no conflict of interest.

*This Direct Submission article had a prearranged editor.

Freely available online through the PNAS open access option.

[1]Present address: Department of Synthetic Chemistry and Biological Chemistry, Graduate School of Engineering, Kyoto University, Kyoto 615-8510, Japan.

[2]To whom correspondence should be addressed. E-mail: yokamura@phys2.med.osaka-u.ac.jp.

This article contains supporting information online at www.pnas.org/lookup/suppl/doi:10.1073/pnas.1203799109/-/DCSupplemental.

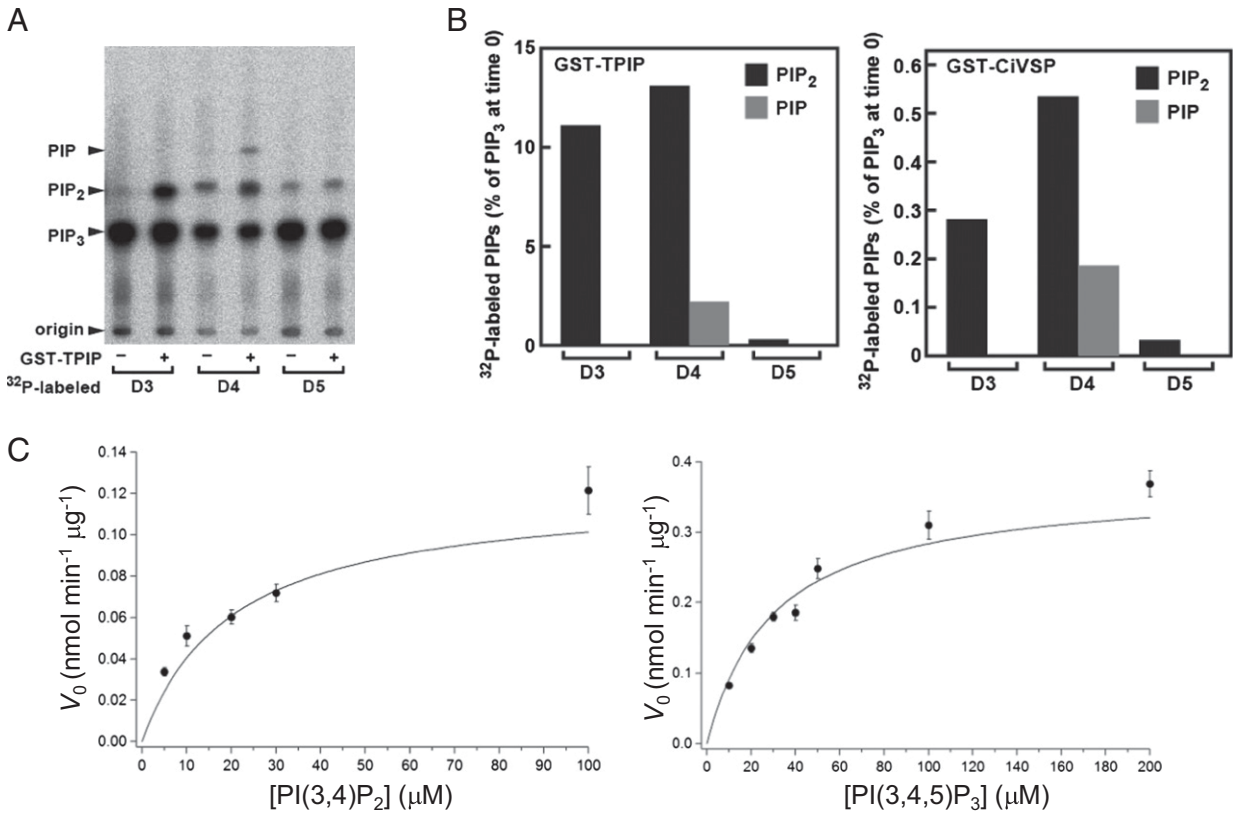

Fig. 1. (*A* and *B*) Purified recombinant TPIP was assayed for phosphatase activity toward PI(3,4,5)P_3 radiolabeled by ^{32}P specifically at D3, D4, or D5 phosphate [PI(**3***,4,5)P_3, PI(3,**4***,5)P_3, or PI(3,4,**5***)P_3]. A representative radio-TLC image (*A*) and quantitative estimation of PI(3,4,5)P_3 phosphatase activity (*B Left*) are shown. Note that ^{32}P-labeled PIP_2 either at D3 or D4 was increased after the reaction, and that formation of PIP was detectable only when PI(3,**4***,5)P_3 was used as substrate. (*B Right*) Ci-VSP displayed similar activity to that of TPIP. (*C*) Malachite green assay with the GST-fused Ci-VSP cytoplasmic region using C16-PI(3,4)P_2. (*Left*) Plot of initial rate against PI(3,4)P_2 concentration. V_{max} and K_m were estimated as 0.121 nmol·min^{-1}·μg^{-1} and 20 μM, respectively. (*Right*) Plot of initial rate against PI(3,4,5)P_3 concentration. V_{max} and K_m were estimated as 0.369 nmol·min^{-1}·μg^{-1} and 30 μM, respectively.

on the D5 position did not give rise to any band shift after incubation with Ci-VSP or TPIP (Fig. 1*B*), indicating that the D3 position phosphate of the inositol ring of PI(3,4,5)P_3 is not removed by VSP. Most of the radiolabeled PI(3,4,5)P_3 was not dephosphorylated in this analysis, as shown in the quantification of radioactive spots (Fig. S1), providing evidence against the possibility that VSP dephosphorylates the D3 position phosphate of PI(3,4,5)P_3 and PI(4,5)P_2 is rapidly dephosphorylated into phosphatidylinositol 4-phosphate [PI(4)P]. These findings indicate that Ci-VSP and TPIP dephosphorylate the 3′ phosphate of PI(3,4)P_2 but not that of PI(3,4,5)P_3.

To confirm the phosphatase activity toward PI(3,4)P_2, a malachite green assay was also performed with the GST-fused polypeptide of the Ci-VSP cytoplasmic region. The results showed that Ci-VSP has enzymatic activity toward PI(3,4)P_2, with K_m = 20 μM and V_{max} = 0.121 nmol·min^{-1}·μg^{-1} (Fig. 1*C* and Table 1). This K_m value was in a similar range to our previously obtained value for PI(3,4,5)P_3 (36 μM) (9), suggesting that VSP has similar affinity toward PI(3,4)P_2 and PI(3,4,5)P_3. The V_{max} value indicates that the turnover rate for PI(3,4)P_2 is about one-third of that for PI(3,4,5)P_3.

Table 1. Kinetic parameters of the malachite green assay of the GST-Ci-VSP polypeptide (residues 248–576) with PI(3,4)P_2 and PI(3,4,5)P_3 as substrate

Substrate	K_m, μM	V_{max}, nmol·min^{-1}·μg^{-1}	K_{cat}, min^{-1}
PI(3,4,5)P_3	30	0.369 ± 0.042	23.4 ± 2.66
PI(3,4)P_2	20	0.121 ± 0.015	7.7 ± 0.95

Measurement was done in six tubes per each concentration of phosphoinositide.

3′ Phosphatase Activity of VSP in Cells. To test whether voltage-dependent dephosphorylation of PI(3,4)P_2 by VSP occurs in live cells, the PI(3,4)P_2 level was monitored in *Xenopus* oocytes by using the GFP-fused pleckstrin homology (PH) domain of tandem PH domain-containing protein (TAPP1) (PH_{TAPP1}-GFP) (19) that selectively binds to PI(3,4)P_2 (20). In oocytes expressing PH_{TAPP1}-GFP with Ci-VSP (Fig. 2*A*), fluorescence intensity increases with depolarization to a level more positive than −40 mV (Fig. 2*B*), consistent with 5′ phosphatase activities toward PI(3,4,5)P_3 (21). Depolarization up to 60 mV led to reduction of GFP fluorescence (Fig. 2*B*), suggesting that the PI(3,4)P_2 level decreases. Pooled data from multiple cells at distinct voltages (Fig. 2*C*) showed a bell-shaped pattern of voltage sensitivity: an increase of fluorescence at depolarizations ranging from −40 mV to 0 mV, saturation of the signal intensity at 30 mV (Fig. 2*C*), and then a decrease from the basal level at 60 mV (Fig. 2*B*). This decrease of the PH_{TAPP1}-GFP signal at 60 mV, compared with the increase at 0 mV, is also illustrated in the bar graph in Fig. S2*E*. The fluorescence change at 60 mV often showed two phases: an early transient increase and a later decrease.

We noticed that oocytes expressing only PH_{TAPP1}-GFP also showed some change of fluorescence upon depolarization (Fig. S2). This activity seemed to depend on some endogenous phosphatase because pervanadate suppressed the fluorescence change (Fig. S2 *C* and *D*). *Xenopus* ortholog VSP mRNA has been

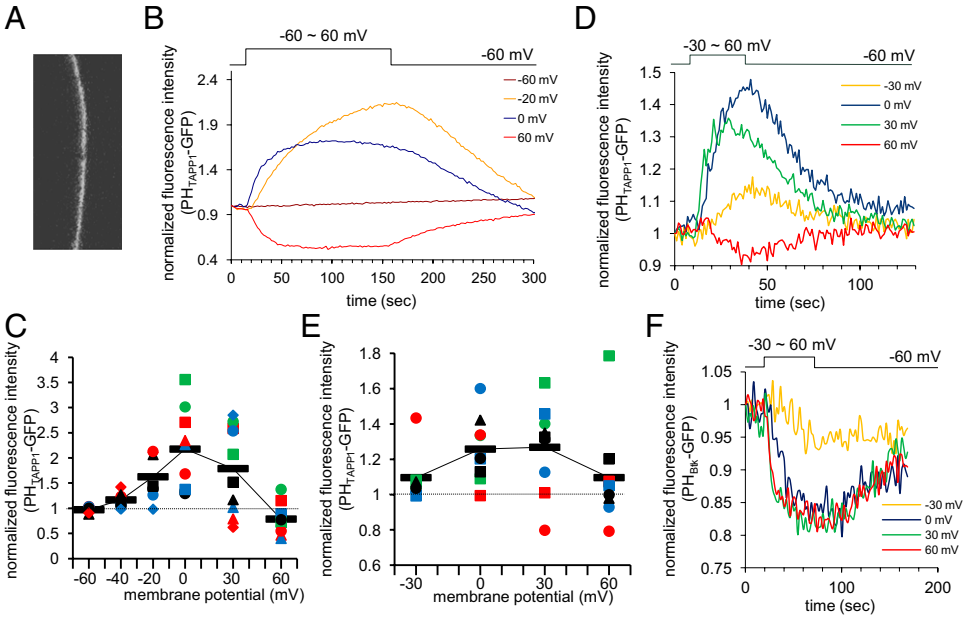

Fig. 2. Confocal microscopic fluorometry of PH_{TAPP1}-GFP fluorescence on Ci-VSP activities. (*A*) Confocal image of PH_{TAPP1}-GFP fluorescence in *Xenopus* oocyte. (*B*) Representative data of fluorescence intensity at four membrane potentials recorded from a single *Xenopus* oocyte expressing Ci-VSP and PH_{TAPP1}-GFP. Fluorescence intensity of GFP in a fixed area containing the contour of *Xenopus* oocyte was measured and plotted against time. Timing of depolarization is indicated above the graph. (*C*) Pooled data of voltage-dependent change in PH_{TAPP1}-GFP fluorescence intensity from multiple cells expressing Ci-VSP (n = 6–10). The mean fluorescence intensity during the last 10 s of depolarizing pulse was normalized by the intensity just before depolarizing pulse in individual cell. Filled red circle represents data shown in *B*. (*D*) Representative data of fluorescence intensity at four membrane potentials recorded from a newt oocyte coexpressing Ci-VSP and PH_{TAPP1}-GFP. (*E*) Pooled data of voltage-dependent change in PH_{TAPP1}-GFP fluorescence intensity from multiple newt oocytes (n = 3–5). Filled triangle represents data shown in *D*. The same symbols represent data from the same cells in *C* and *E*. (*F*) Change of PH_{Btk}-GFP fluorescence intensity upon depolarization to an indicated level. Oocytes were microinjected with cRNAs encoding Ci-VSP, PH_{TAPP1}-GFP, and p110CAAX-K227E and preincubated with 8 μM insulin. Voltage step was applied for 50 s from a holding potential of −60 mV in ND96.

reported to be present in gonads (12). The change of PH_{TAPP1}-GFP in the absence of VSP differs from that based on heterologously expressed VSP in that the fluorescence signal does not increase at less than 10 mV and that it shows no reduction of fluorescence at high depolarization.

We also used oocytes from the Japanese newt *Cynops pyrrhogaster* as a system for heterologous expression (22). Newt oocytes overexpressing only PH_{TAPP1}-GFP exhibited no voltage-dependent change of fluorescence (Fig. S3). Newt oocytes expressing Ci-VSP and PH_{TAPP1}-GFP recapitulated phenotypes of *Xenopus* oocytes with Ci-VSP and PH_{TAPP1}-GFP: they showed an increase of fluorescence signal with mild depolarization, saturation, and sometimes reduction of signal at higher depolarization (Fig. 2 *D* and *E*). This finding verifies that changes of PH_{TAPP1}-GFP upon activation of VSP phosphatases observed in *Xenopus* oocytes were not significantly affected by endogenous enzyme activities. Variations in voltage-dependent profile of change of PH_{TAPP1}-GFP signal were more remarkable in newt oocytes than in *Xenopus* oocytes, probably because of larger variations of expressed Ci-VSP proteins in cell membranes. In later studies, we used *Xenopus* oocytes.

To test whether the above pattern of $PI(3,4)P_2$ change could be attributable to a possible bell-shaped voltage dependence of phosphatase activity toward $PI(3,4,5)P_3$, $PI(3,4,5)P_3$ level was monitored by the GFP-fused PH domain from Btk (PH_{Btk}-GFP) as previously done (18). To increase resting $PI(3,4,5)P_3$ level, a constitutively active, membrane-bound version of PI3-kinase, p110CAAX-K227E, was coexpressed. In the same oocytes, reduction was more prominent at higher voltage levels (Fig. 2*F*), negating the idea of a bell-shaped voltage dependence of D5 dephosphorylation of $PI(3,4,5)P_3$.

To explore whether the ability to dephosphorylate $PI(3,4)P_2$ is a conserved feature among VSP orthologs, full-length human VSP (TPIP) (13) was cloned, and cDNA encoding a chimeric protein comprising the VSD from Ci-VSP and the cytoplasmic region from TPIP was constructed (Fig. S4). This chimeric protein, Ci-Hs-VSP, showed voltage-dependent $PI(4,5)P_2$ phosphatase activities (Fig. S5). As monitored by PH_{TAPP1}-GFP, Ci-Hs-VSP showed a response similar to that of Ci-VSP: an increase at 0 mV and a decrease at 60 mV (Fig. S6). The magnitude of sensing charges (Figs. S6*C* and S7) were not markedly different between Ci-VSP and Ci-Hs-VSP, suggesting similar levels of surface expression. The relative fluorescence change measured at 0 mV, standardized by the magnitude of the sensing charges in individual oocytes, showed similar values for Ci-VSP and Ci-Hs-VSP (Fig. S6*D*).

$PI(3,4)P_2$ Decrease upon Activation of VSPs Is Not Secondary to Depletion of $PI(4,5)P_2$. The level of $PI(3,4)P_2$ is maintained by the equilibrium among distinct transitions, including production from $PI(3,4,5)P_3$ or PI(4)P and dephosphorylation of $PI(3,4)P_2$. The decrease of $PI(3,4)P_2$ upon VSP activities could indirectly be brought about by phosphatase activities of VSPs toward $PI(4,5)P_2$ and $PI(3,4,5)P_3$ (9, 21). $PI(4,5)P_2$ is the source of $PI(3,4,5)P_3$ that then gives rise to $PI(3,4)P_2$ through dephosphorylation of D5 phosphate. It has also been shown that the putative $PI(4,5)P_2$ binding site in the linker between the VSD and the enzyme region is critical for the interaction between the two domains (23, 24), raising the possibility that binding of $PI(4,5)P_2$ to the linker regulates the function of VSP and thus the depletion of $PI(4,5)P_2$ might suppress VSP phosphatase activity.

To test these possibilities, two modified versions of VSPs with reduced $PI(4,5)P_2$ phosphatase activity were used. Glycine 365 and glutamic acid 411 in Ci-VSP are highly conserved residues in the active site (Fig. 3*A*). Glycine 365 is important for robust $PI(4,5)P_2$ phosphatase activity of Ci-VSP (9), and glutamic acid 411 is important for determining substrate specificity, in

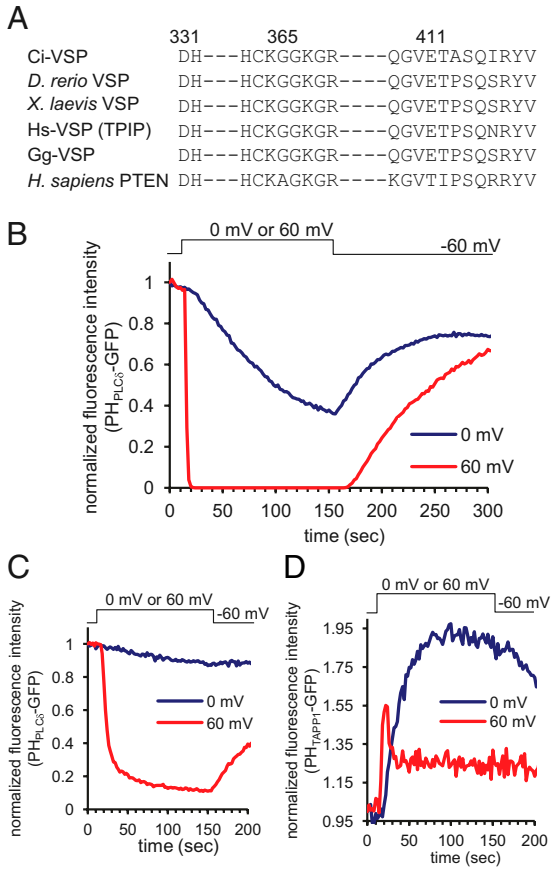

Fig. 3. (*A*) Sequence alignment of amino acid among several VSPs and human PTEN in the phosphatase domain. (*B*) $PH_{PLC\delta}$-GFP fluorescence at 0 mV (blue) or 60 mV (red) depolarization with wild-type Ci-VSP. (*C*) $PH_{PLC\delta}$-GFP fluorescence with G365A/E411T mutant. It shows milder reduction of $PI(4,5)P_2$ level than wild-type Ci-VSP. (*D*) Change of fluorescence from PH_{TAPP1}-GFP upon depolarization to 0 mV or 60 mV.

particular, suppressing phosphatase activity toward $PI(3,5)P_2$ (10). In vitro malachite green assays show that the double mutant G365A/E411T exhibits reduced phosphatase activity toward $PI(4,5)P_2$ but retains activity toward $PI(3,4,5)P_3$ (Fig. S8*B*). Confocal microscopic fluorometry of the GFP-fused PH domain of phospholipase Cδ ($PH_{PLC\delta}$-GFP) fluorescence shows less decrease of signal with G365A/E411T than with wild-type Ci-VSP (Fig. 3 *B* and *C*). When G365A/E411T Ci-VSP was coexpressed with PH_{TAPP1}-GFP in *Xenopus* oocytes, an increase of fluorescence signal was observed at 0 mV, indicating that G365A/E411T retains 5′ phosphatase activity toward $PI(3,4,5)P_3$. In addition, a late phase of reduction of $PI(3,4)P_2$ level followed a transient increase of fluorescence intensity at 60 mV (Fig. 3*D*). These findings are inconsistent with the idea that depletion of $PI(4,5)P_2$ indirectly decreases $PI(3,4)P_2$ level upon depolarization-induced VSP activities. These results also indicate that the two sites, G365 and E411, cannot fully account for distinct substrate specificity of VSPs other than PTEN.

We also used the chick ortholog (16) (designated as Gg-VSP) that shows reduced phosphatase activity toward $PI(4,5)P_2$ than Ci-VSP does but retains $PI(3,4,5)P_3$ phosphatase activity. In the malachite green assay (Fig. S8*A*), the cytoplasmic region of Gg-VSP exhibits lower $PI(4,5)P_2$ phosphatase activity than $PI(3,4,5)P_3$ phosphatase activity. To standardize the voltage sensitivity and surface expression level between Ci-VSP and Gg-VSP, the VSD of Ci-VSP was fused to the enzyme region of Gg-VSP (designated as Ci-Gg-VSP). Under conditions with similar surface expression between Ci-VSP and Ci-Gg-VSP, Ci-Gg-VSP showed a much smaller decrease of $PH_{PLC\delta}$-GFP signal than Ci-VSP did (Figs. 3*B* and 4 and Fig. S9). At 60 mV, the signal is markedly reduced at 10 s after depolarization (Fig. 3*B*) in Ci-VSP, whereas a persistent component of fluorescence during depolarization is seen with Ci-Gg-VSP. On the other hand, a similar depolarization-dependent decrease of the PH_{TAPP1}-GFP signal was observed at 60 mV in Ci-Gg-VSP as in Ci-VSP (Fig. 4*F*). The standardized magnitude of fluorescence signal, as estimated in individual oocytes by dividing fluorescence change per sensing charge (Fig. 4 *D* and *E*), did not differ markedly between Ci-Gg-VSP and Ci-VSP (about 65% of Ci-VSP) for PH_{TAPP1}-GFP but did differ largely between Ci-Gg-VSP and Ci-VSP for $PH_{PLC\delta}$-GFP (about 15% of Ci-VSP).

In summary, VSP has dephosphorylation activity toward $PI(3,4)P_2$, resulting in a reciprocal change of the level of $PI(3,4)P_2$ that depends on the level of voltage (Fig. 4*G*).

Discussion

Our previous results of in vitro measurements of Ci-VSP suggested that VSP has phosphatase activity toward $PI(3,4)P_2$ (9, 10). In the present study, we showed that VSP has 3′ phosphate phosphatase activity toward $PI(3,4)P_2$, both by in vitro measurements and by live-cell imaging. It is unlikely that the voltage-dependent decrease of $PI(3,4)P_2$ in live cells could be indirectly induced by alterations of other phosphoinositide species. Two versions of VSPs, G365A/E411T Ci-VSP and a chimeric protein harboring the cytoplasmic region of chick VSP (Ci-Gg-VSP), show reduced phosphatase activities toward $PI(4,5)P_2$. These exhibited a voltage-dependent decrease of $PI(3,4)P_2$ as did the wild-type Ci-VSP. Detailed quantitative analyses are hampered by the presence of unknown endogenous voltage-sensitive activities that increased the level of $PI(3,4)P_2$, which could be because of endogenous VSP activities given that *Xenopus* gonads have transcripts of two VSP genes (12). However, these endogenous activities were resistant to antisense DNAs against *Xenopus* VSP transcripts. Newt oocytes that do not exhibit endogenous voltage-sensitive changes in the level of $PI(3,4)P_2$ still showed similar bell-shaped voltage dependence of the level of $PI(3,4)P_2$ as in *Xenopus* oocytes.

How can the 3′ phosphatase activity of the VSP be interpreted in light of recently resolved structural information (10)? The substrate-binding pocket of VSP is slightly smaller than that of PTEN, at least in part because of the presence of glutamic acid at residue 411 instead of threonine (which is the residue in the corresponding site of PTEN) (10). Modeling of the docking of inositol 1,3,4,5-tetrakisphosphate [$Ins(1,3,4,5)P_3$] suggests that the residue histidine 332 interacts with the 4′ phosphate to stabilize binding of phosphoinositides that contain 4′ phosphate such as $PI(4,5)P_2$, $PI(3,4)P_2$, and $PI(3,4,5)P_3$ (10). $PI(4,5)P_2$ and $PI(3,4,5)P_3$ present their 5′ phosphate of the inositol ring on the side of cysteine 363 in the active center for dephosphorylation. This orientation is more favorable for docking of $PI(3,4,5)P_3$ than the flipped orientation with the axis of the 1′ to 4′ position is in part because of steric hindrance and/or electrostatic repulsion by E411. Unlike $PI(3,4,5)P_3$, $PI(3,4)P_2$ may be able to dock to the substrate-binding pocket in the flipped orientation where the 3′ phosphate could position next to cysteine 363, with the 4′ phosphate positioning next to histidine 332.

Interestingly, the decrease of $PI(3,4)P_2$ was observed only at high voltages. $PI(4,5)P_2$ binding to the phosphoinositide-binding motif between the VSD and the cytoplasmic region has been suggested by previous studies to play role in coupling the VSD to the cytoplasmic region (24). Two versions of VSPs with reduced $PI(4,5)P_2$ phosphatase activities showed saturation or decrease of $PI(3,4)P_2$ level upon large depolarization, and the level of $PI(3,4,5)P_3$ monitored by PH_{Btk}-GFP did not show blunted phosphatase activity at high depolarization, ruling out the possibility that a potential regulatory role of $PI(4,5)P_2$ in VSP

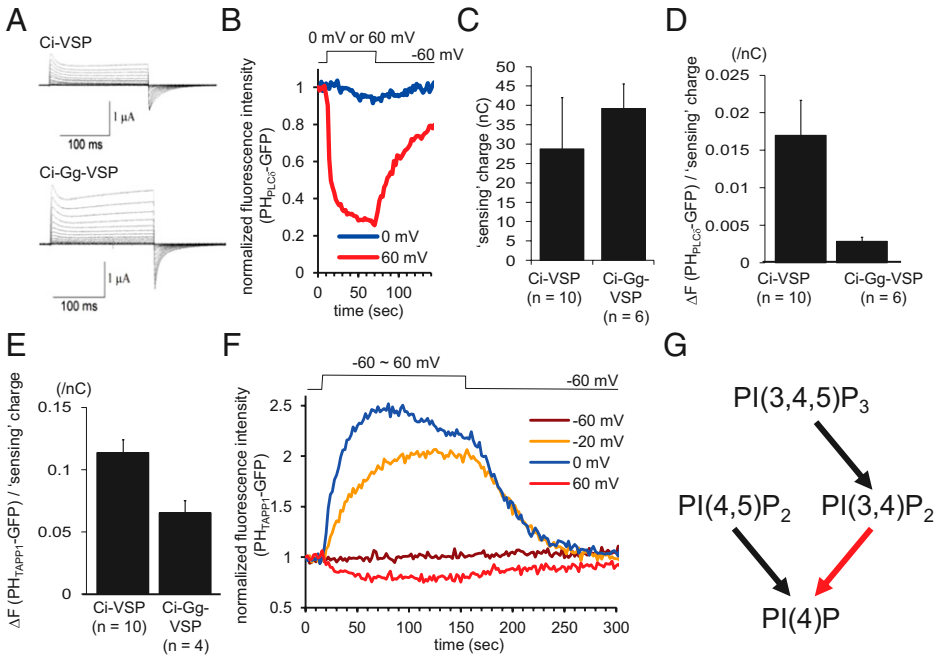

Fig. 4. Decrease of PI(3,4)P_2 at 60 mV depolarization in *Xenopus* oocyte expressing ascidian–chick VSP chimera (Ci-Gg-VSP). (*A*) Sensing currents of Ci-Gg-VSP (*Lower*), a chimera of Ci-VSP VSD and chick VSP phosphatase region compared with those of Ci-VSP (*Upper*). (*B*) PI(4,5)P_2 phosphatase activities of Ci-Gg-VSP by confocal microscopy measurements of PH$_{PLCδ}$-GFP fluorescence upon depolarization to 0 mV and 60 mV. Note that Ci-Gg-VSP has milder PI(4,5)P_2 phosphatase activity than Ci-VSP (Fig. 3*B*). (*C*) Magnitude of sensing charges. Sensing charges were obtained by integrating OFF sensing currents that are evoked by repolarization to −60 mV after 200-ms depolarization to 140 mV. (*D*) Extent of voltage-induced change of PH$_{PLCδ}$-GFP fluorescence at 0 mV, standardized by sensing charge (reflecting the surface expression level) of VSP. Sensing currents and PH$_{PLCδ}$-GFP fluorescence were measured from the same cells. The maximum intensity during depolarizing pulse normalized by the fluorescence intensity just before depolarization was divided by the magnitude of sensing currents in individual cells. (*E*) Magnitude of voltage-dependent change of fluorescence of PH$_{TAPP1}$-GFP standardized by the magnitude of sensing currents in individual cells. (*F*) Time course of fluorescence from PH$_{TAPP1}$-GFP upon depolarization to four distinct voltage levels. Ci-Gg-VSP shows decrease of PI(3,4)P_2 signal at 60 mV. (*G*) Scheme of VSP phosphatase activities. The transition proposed in this study is in red.

enzymatic activities underlies the bell-shaped voltage dependence of PI(3,4)P_2 change. Then how is dephosphorylation of PI(3,4)P_2 seen more remarkably at higher depolarization? One possibility is that PI(3,4,5)P_3 and PI(3,4)P_2 compete for the substrate-binding site of VSP and the relative availability of PI(3,4)P_2 versus PI(3,4,5)P_3 as substrate for dephosphorylation by VSP is biased by membrane potential. Given that the headgroup of PI(3,4,5)P_3 has two more negative charges than that of PI(3,4)P_2, the effect of electric field across the cell membrane on the phosphoinositide headgroup will be more potent for PI(3,4,5)P_3 than for PI(3,4)P_2. Alternatively, substrate preference could be based on the distinct conformation of the VSP's enzyme region coupled to the distinct activated state of the VSD. More studies will be necessary to reveal mechanisms by which substrate preference depends on membrane potential.

PI(3,4)P_2 plays a key role in cell morphology and cell adhesion by regulating signaling in the formation of podosomes (25) or lamellipodia through binding to Tks5/FISH (26), lamellipodin (27, 28), and TAPP1 (19). VSP/TPTE is expressed in testis of ascidian, chick, mouse, and human. VSP is also expressed in blood cells, the nervous system, and epithelium of the developing intestine of ascidian (29) and in the epithelium of chick kidney (16). Patterns of membrane-potential changes may lead to alteration of cell morphology in these VSP-expressing cells, and the bidirectionality of the regulation of PI(3,4)P_2 levels may be important for fine-tuning cell morphology that depends on membrane potential. Ci-VSP is also expressed in sperm where membrane-potential change takes place upon exposure to an egg-derived chemoattractant called sperm activating and attracting factor (SAAF) (30). Future studies examining membrane-potential changes in VSP-expressing cells such as sperm, blood cells, or developing cells, are necessary to gain insights into physiological roles of activities of VSP.

Materials and Methods

cDNA Cloning and Plasmids. For human VSP (TPIP) cDNA, human testis RNA purchased from Clontech was reverse-transcribed, and cDNA was amplified by PCR. Ci-Hs-VSP (ascidian–human VSP) chimera was generated by using the cDNA encoding residues 1–257 of Ci-VSP and 215–522 of TPIP as a template and subcloned into the XhoI/NotI site of pSD64 vector (kindly gifted by Terry Snutch, University of British Columbia, Vancouver, Canada) for *Xenopus* oocyte expression. The Ci-Gg-VSP (ascidian–chick VSP) chimera was generated by using the cDNA encoding residues 1–257 of Ci-VSP and 197–511 of Gg-VSP and subcloned into pSD64 vector. Point mutants of G365A/E411T into Ci-VSP were generated by PCR (QuikChange kit; Stratagene). The PH$_{TAPP1}$-GFP construct was made by modifying the PH$_{TAPP1}$-YFP construct kindly provided by Dario Alessi (Medical Research Council, Dundee, United Kingdom). A constitutively active, membrane-bound form of PI3-kinase was constructed by introduction of a mutation of K227E into p110CAAX (p110CAAX-K227E; kindly gifted by Thomas Franke, New York University, New York, NY) subcloned into pSD64.

In Vitro Phosphatase Assay. For malachite green assay, dipalmitoyl-phosphoinositides (Wako and Echelon Biosciences) and phosphatidylserine (Sigma) were used. The reactions were initiated by the addition of 2 μg of GST-Ci-VSP (residues 248–576) and incubated at 23 °C. BIOMOL Green reagent was added to the supernatants, and OD_{620} was measured. Time-dependent activity was measured with different substrate doses up to 200 μM. Data were fit with IgorPro. Initial rate, V_0, of Ci-VSP–catalyzed dephosphorylation of PI(3,4,5)P_3 and PI(3,4)P_2 was determined from reactions with various concentrations of substrate. Data were fit by the equation: $V_0 = V_{max}$[substrate]/(K_m + [substrate]).

TLC Assay. For TLC assay, assay buffer (Tris·HCl and DTT) was added to the mixture of phosphatidylserine, nonradioactive PI(3,4,5)P_3, and radioactive PI(3,4,5)P_3. [D3-^{32}P]PI(3,4,5)P_3 was obtained by incubating dipalmitoyl-

$PI(4,5)P_2$ with [γ-^{32}P]ATP in the presence of PI3-kinase, FLAG-tagged iSH2-p110α. [D4-^{32}P]$PI(3,4,5)P_3$ and [D5-^{32}P]$PI(3,4,5)P_3$ were prepared from [D4-^{32}P]$PI(4,5)P_2$ and [D5-^{32}P]$PI(4,5)P_2$, respectively (see *SI Materials and Methods* for more detailed descriptions). Reaction was performed with purified GST-Ci-VSP at 23 °C.

Electrophysiology and Live-Cell Imaging of Phosphoinositides. *Xenopus laevis* and Japanese newt, *C. pyrrhogaster*, were anesthetized by immersion in water containing 0.1–0.2% Tricaine. Experiments were performed according to the guidelines of the Animal Research Committees of the Graduate School of Medicine of Osaka University. The oocytes were incubated at 18 °C in ND96 solution (31).

Sensing current was recorded under the two-electrode voltage clamp with a "bath-clamp" amplifier (OC-725C; Warner Instruments) (7). Linear and symmetrical current were subtracted by a *P/*–8 procedure. Stimulation and data acquisition were performed with Digidata 1440A AD/DA converter with pCLAMP software (Molecular Devices). The bath solution contained 96 mM *N*-methyl-D-glucamine-methanesulfonate, 3 mM $MgCl_2$, and 5 mM Hepes (pH 7.4) or ND96. The level of $PI(4,5)P_2$ or $PI(3,4)P_2$ was monitored by imaging of $PH_{PLC\delta}$-GFP or PH_{TAPP1}-GFP, respectively, in *Xenopus* oocyte and newt oocyte with a confocal microscopy system (FV300; Olympus). The level of $PI(3,4,5)P_3$ was monitored by imaging of PH_{Btk}-GFP. The resting $PI(3,4,5)P_3$ level was increased by heterologously expressing a membrane-bound, constitutively active form of PI3-kinase, p110CAAX-K227E, and by preincubation with 8 μM insulin. After insertion of microelectrodes, cell was kept to −60 mV for more than 1 min for phosphoinositide levels to reach steady state.

Note Added in Proof. A decline of PH_{TAPP1}-GFP fluorescence upon activities of Ci-VSP has been reported also in a recent paper (Liu at al. (2012) A glutamate switch controls voltage-sensitive phosphatase function. *Nature Struct and Mol Biol*, 10.1038/nsmb.2289).

ACKNOWLEDGMENTS. We thank Dr. D. Alessi for providing the TAPP1 plasmid, Dr. M. Fukuda for providing the PH_{Btk} plasmid, and Dr. T. Franke for providing the p110CAAX plasmid. We also thank Dr. Y. Iwao for advice on newts, Dr. L. Jaffe for reading the manuscript and for discussion, and Dr. Y. Mori for encouragement. This work was supported by grants from the Japan Ministry of Education, Culture, Sports, Science, and Technology (MEXT) (to Y.O., T.K., S.S., S.T., and T.S.), the Human Frontier Science Program (to Y.O.), the Targeted Proteins Research Program from MEXT (to Y.O.), and the General Collaborative Project by the National Institute for Physiological Sciences, Okazaki, Japan (to Y.O., T.S., and K.J.H.).

1. Sasaki T, et al. (2009) Mammalian phosphoinositide kinases and phosphatases. *Prog Lipid Res* 48:307–343.
2. Liu Y, Bankaitis VA (2010) Phosphoinositide phosphatases in cell biology and disease. *Prog Lipid Res* 49:201–217.
3. Maehama T, Taylor GS, Dixon JE (2001) PTEN and myotubularin: Novel phosphoinositide phosphatases. *Annu Rev Biochem* 70:247–279.
4. Di Cristofano A, Pandolfi PP (2000) The multiple roles of PTEN in tumor suppression. *Cell* 100:387–390.
5. Rossi DJ, Weissman IL (2006) *Pten*, tumorigenesis, and stem cell self-renewal. *Cell* 125: 229–231.
6. Butler M, et al. (2002) Specific inhibition of PTEN expression reverses hyperglycemia in diabetic mice. *Diabetes* 51:1028–1034.
7. Murata Y, Iwasaki H, Sasaki M, Inaba K, Okamura Y (2005) Phosphoinositide phosphatase activity coupled to an intrinsic voltage sensor. *Nature* 435:1239–1243.
8. Okamura Y, Dixon JE (2011) Voltage-sensing phosphatase: Its molecular relationship with PTEN. *Physiology (Bethesda)* 26:6–13.
9. Iwasaki H, et al. (2008) A voltage-sensing phosphatase, Ci-VSP, which shares sequence identity with PTEN, dephosphorylates phosphatidylinositol 4,5-bisphosphate. *Proc Natl Acad Sci USA* 105:7970–7975.
10. Matsuda M, et al. (2011) Crystal structure of the cytoplasmic phosphatase and tensin homolog (PTEN)-like region of *Ciona intestinalis* voltage-sensing phosphatase provides insight into substrate specificity and redox regulation of the phosphoinositide phosphatase activity. *J Biol Chem* 286:23368–23377.
11. Hossain MI, et al. (2008) Enzyme domain affects the movement of the voltage sensor in ascidian and zebrafish voltage-sensing phosphatases. *J Biol Chem* 283:18248–18259.
12. Ratzan WJ, Evsikov AV, Okamura Y, Jaffe LA (2011) Voltage sensitive phosphoinositide phosphatases of *Xenopus*: Their tissue distribution and voltage dependence. *J Cell Physiol* 226:2740–2746.
13. Walker SM, Downes CP, Leslie NR (2001) TPIP: A novel phosphoinositide 3-phosphatase. *Biochem J* 360:277–283.
14. Wu Y, et al. (2001) PTEN 2, a Golgi-associated testis-specific homologue of the PTEN tumor suppressor lipid phosphatase. *J Biol Chem* 276:21745–21753.
15. Leslie NR, Yang X, Downes CP, Weijer CJ (2007) PtdIns(3,4,5)P(3)-dependent and -independent roles for PTEN in the control of cell migration. *Curr Biol* 17:115–125.
16. Neuhaus H, Hollemann T (2009) Kidney specific expression of cTPTE during development of the chick embryo. *Gene Expr Patterns* 9:568–571.
17. Zhang L, Lee JK, John SA, Uozumi N, Kodama I (2004) Mechanosensitivity of GIRK channels is mediated by protein kinase C-dependent channel-phosphatidylinositol 4,5-bisphosphate interaction. *J Biol Chem* 279:7037–7047.
18. Murata Y, Okamura Y (2007) Depolarization activates the phosphoinositide phosphatase Ci-VSP, as detected in *Xenopus* oocytes coexpressing sensors of PIP2. *J Physiol* 583:875–889.
19. Dowler S, et al. (2000) Identification of pleckstrin-homology-domain-containing proteins with novel phosphoinositide-binding specificities. *Biochem J* 351:19–31.
20. Kimber WA, et al. (2002) Evidence that the tandem-pleckstrin-homology-domain-containing protein TAPP1 interacts with Ptd(3,4)P2 and the multi-PDZ-domain-containing protein MUPP1 in vivo. *Biochem J* 361:525–536.
21. Halaszovich CR, Schreiber DN, Oliver D (2009) Ci-VSP is a depolarization-activated phosphatidylinositol-4,5-bisphosphate and phosphatidylinositol-3,4,5-trisphosphate 5′-phosphatase. *J Biol Chem* 284:2106–2113.
22. Kobayashi S, Iio H, Aoshima H (1986) New translation system of mRNA coding for neurotransmitter receptors using oocytes of the newt, *Cynops pyrrhogaster*. *Brain Res* 387:93–96.
23. Villalba-Galea CA, Miceli F, Taglialatela M, Bezanilla F (2009) Coupling between the voltage-sensing and phosphatase domains of Ci-VSP. *J Gen Physiol* 134:5–14.
24. Kohout SC, et al. (2010) Electrochemical coupling in the voltage-dependent phosphatase Ci-VSP. *Nat Chem Biol* 6:369–375.
25. Symons M (2008) Cell biology: Watching the first steps of podosome formation. *Curr Biol* 18:R925–R927.
26. Oikawa T, Itoh T, Takenawa T (2008) Sequential signals toward podosome formation in NIH-src cells. *J Cell Biol* 182:157–169.
27. Bae YH, et al. (2010) Profilin1 regulates PI(3,4)P2 and lamellipodin accumulation at the leading edge thus influencing motility of MDA-MB-231 cells. *Proc Natl Acad Sci USA* 107:21547–21552.
28. Krause M, et al. (2004) Lamellipodin, an Ena/VASP ligand, is implicated in the regulation of lamellipodial dynamics. *Dev Cell* 7:571–583.
29. Ogasawara M, Sasaki M, Nakazawa N, Nishino A, Okamura Y (2011) Gene expression profile of Ci-VSP in juveniles and adult blood cells of ascidian. *Gene Expr Patterns* 11: 233–238.
30. Izumi H, Márián T, Inaba K, Oka Y, Morisawa M (1999) Membrane hyperpolarization by sperm-activating and -attracting factor increases cAMP level and activates sperm motility in the ascidian *Ciona intestinalis*. *Dev Biol* 213:246–256.
31. Goldin AL (1992) Maintenance of *Xenopus laevis* and oocyte injection. *Methods Enzymol* 207:266–279.